Available online at www.sciencedirect.com
SCIENCE DIRECT®
Carbohydrate Polymers 53 (2003) 169–182
Carbohydrate Polymers
www.elsevier.com/locate/carbpol

In-line determination of plasticized wheat starch viscoelastic behavior: impact of processing

O. Martin[a], L. Averous[a,*], G. Della Valle[b]

[a]*Centre d'Etudes et de Recherche en Materiaux et Emballage (CERME): Materials and Packaging Research Centre (ESIEC), UMR INRA/Universite de Reims Champagne-Ardenne (URCA) (FARE), B.P. 1029, 51686 Reims Cedex 2, France*
[b]*INRA, B.P. 71627, 44316 Nantes Cedex 3, France*

Received 1 August 2002; revised 19 December 2002; accepted 23 December 2002

Abstract

In-line slit and capillary die viscometers were specially designed to study the viscoelastic behavior of plasticized wheat starch under low-hydrated conditions. A wide range of shear rates could be obtained by the use of different die geometries. The effects of temperature (110–150 °C), glycerol (10–35%) and moisture contents (0–20%) were studied. The influence of the specific mechanical energy (SME) (100–650 kWh/t) applied to the products was also accounted for. In the range of extrusion conditions, the viscosity data of starch melts followed the classical power-law behavior. A general rheological model was derived from experimental results. Discrepancies of viscosity values found between in-line viscometry results and those of a pre-shearing rheometer, the Rhéoplast®, could be explained by carefully taking into account the temperature and SME conditions. The impact of processing in regards to the starch transformation was investigated through intrinsic viscosity measurements and thermal analysis. The elastic properties of starch melts were also assessed through the analysis of entrance and exit pressures data.

Keywords: Plasticized starch; Viscometry; Thermomechanical treatment

1. Introduction

In the past decade, the use of starch resources in non-food applications has considerably developed in order to find substitutes to petroleum-based plastics, because of growing environmental issues. The potential development of starch-based plastics involves a better understanding of the starch transformation using conventional polymer processing operations (Doane, 1992). In addition, the knowledge of the viscous behavior of low-moisture molten starch is required to better control the quality of extruded products as well as to determine optimal processing conditions.

The extrusion and viscous behavior of molten starch is known to depend on temperature, moisture content and thermomechanical treatment (McMaster, Senouci, & Smith, 1987; Padmanabhan & Bhattacharya 1991; Parker, Ollett, Lai-Fook, & Smith, 1990a; Parker, Ollett, & Smith, 1990b). Viscosity data and rheological models that take into account these variables have been reported in literature. Table 1 summarizes the main rheological studies performed on starch, including the measurement technique and models used. They all report a thermoplastic behavior of low hydrated starch, within a two orders of magnitude shear-rate range, with an Arrhenius dependence on temperature and similar for moisture content. Conversely, structural modifications of starch, also affecting the viscosity of product, is reflected differently by specific mechanical energy (SME), the screw speed (N), or even the extruder barrel pressure (P_b), which depend on the machine characteristics (see equations of Table 1). This discrepancy underlines the need for ascertaining the dependence of starch melt viscosity upon structural factors or variables directly involved in its transformation. Some authors have introduced terms relating the modification of starch, such as conversion, degree of transformation, or extent of degradation (Barrès, Vergnes, Tayeb, & Della Valle, 1990; Colonna, Tayeb, & Mercier, 1989; Davidson, Paton, Diosady, & Larocque, 1984a; Davidson, Paton, Diosady, & Rubin, 1984b; Zheng & Wang, 1994). Lai and Kokini (1990) studied the rheological

* Corresponding author. Tel.: +33-3-26-913-914; fax: +33-3-26-913-803.
E-mail address: luc.averous@univ-reims.fr (L. Averous).

0144-8617/03/$ - see front matter © 2003 Elsevier Science Ltd. All rights reserved.
doi:10.1016/S0144-8617(03)00040-7

Table 1
Chronology of the published studies on molten starches and rheological models used

Reference	Product	Experimental set-up	Rheological model[a]	Temperature (°C)	Moisture content (%)	Conditions
Harper et al. (1971)	Cereal dough	Single-screw extruder + cylindrical die	$\eta = K_0 \exp(\Delta E/RT)\exp(k\mathrm{MC})\dot{\gamma}^{n-1}$, $\Delta E/R = 2482$ K; $k = -0.079$	67–100	25–30	–
Cervone and Harper (1978)	Corn flour	Single-screw extruder + slit die	$\eta = K_0 \exp(\Delta E/RT)\exp(k\mathrm{MC})\dot{\gamma}^{n-1}$, $\Delta E/R = 4388$ K; $k = -0.101$	90–150	22–30	10–100 rpm, $10^1 < \dot{\gamma} < 10^3$ s^{-1}
Fletcher et al. (1985)	Corn grits	Single-screw extruder + slit die rheometer	$\eta = K_0 \exp(\Delta E/RT)\exp(k\mathrm{MC})\dot{\gamma}^{n-1}$, $\Delta E/R = 3969$ K; $k = -0.03$	153–168	15–18	50–200 rpm, $10^1 < \dot{\gamma} < 10^3$ s^{-1}
Vergnes and Villemaire (1987)	Corn starch	Pre-shearing rheometer Rhéoplast®	$\eta = K_0 \exp(E/RT - \alpha\mathrm{MC} - \beta W)\dot{\gamma}^{n-1}$, $E/R = 4250$ K; $\alpha = 10.6$; $\beta = 0.088$	110–170	26–49	200–600 rpm, $10^1 < \dot{\gamma} < 10^3$ s^{-1}
Senouci and Smith (1988a)	Corn starch	Twin-screw extruder + slit die rheometer	$\eta = K_0 N^{-\alpha} \exp(\Delta E/RT)\exp(k\mathrm{MC})\dot{\gamma}^{n-1}$, $\Delta E/R = 2834$ K; $k = -0.032$; $\alpha = 0.541$	100–140	20–31.5	100–250 rpm, $10^1 < \dot{\gamma} < 10^3$ s^{-1}
Padmanabhan and Bhattacharya (1991)	Corn meal	Single-screw extruder + slit die viscometer	$\eta = m\dot{\gamma}^{n-1} \exp(\Delta E/RT + \alpha\mathrm{MC} + gP_b)$, $\Delta E/R = 2726$ K; $\alpha = -1.99$; $g = 3.5 \times 10^{-8}$	150–180	25–45	80–240 rpm, $10^2 < \dot{\gamma} < 10^3$ s^{-1}
Willett et al. (1995)	Corn starch	Single-screw extruder + capillary die viscometer	$\eta = K(T_0)\exp[E/RT - \alpha\mathrm{MC}]\dot{\gamma}^{n-1}$, $E/R = 8500$ K; $\alpha = 12.6$	110–130	15–30	1–60 rpm, $10^1 < \dot{\gamma} < 10^3$ s^{-1}
Della Valle et al. (1996)	Corn starch (0–70% amylose contents)	Twin-screw extruder + Rheopac	$\eta = K_0 \exp[E/RT - \alpha\mathrm{MC} - \beta\mathrm{SME}]\dot{\gamma}^{n-1}$, $E/R = 6140$ K; $\alpha = 18.6$; $\beta = 2.1 \times 10^{-3}$	100–185	20–36	80–240 rpm, $10^1 < \dot{\gamma} < 10^3$ s^{-1}

[a] All variables are expressed in the SI units system (K in Pa s, E/R in Kelvin, β in (kWh/t)$^{-1}$ and g in Pa^{-1}). k and α are dimensionless coefficients.

properties of high amylose (70%) and high amylopectin (98%) corn starches, and showed the strong influence of the processing history undergone by products prior viscosity measurements. Zheng and Wang (1994) identified the contribution of shear and thermal energies in the conversion of waxy corn starch. Della Valle, Boché, Colonna, and Vergnes (1995) and Della Valle, Colonna, Patria, and Vergnes (1996) took into account the transformation of starch and the resulting macromolecular degradation, evaluated by chromatography (SEC profiles) and intrinsic viscosity, by confirming the importance of the term noted β. Plasticizing starch with glycerol adds complexity to the system. Recently, Aichholzer and Fritz (1998) described the flow properties of glycerol processed thermoplastic starch as a function of compounding parameters, melt temperature and content of additives, but did not directly incorporate the effect of starch transformation in their model. To the best of our knowledge, there is little data available on plasticized wheat starch (PWS). Moreover, the impact of the processing conditions on the rheological behavior of glycerol plasticized starch systems needs to be documented. A common difficulty of such studies is that a thermomechanical treatment is needed to obtain a homogeneous molten starch phase prior to measurement and that traditional rheometry (rotational, capillary) is not appropriate for the study of the rheological behavior of low-moisture starches. Moreover, it is of great advantage to be able to measure the viscosity behavior of starch melts directly after processing in the extruder. In that respect, extruder-fed slit rheometry is well adapted (Bastioli, Bellotti, & Rallis, 1994; Senouci & Smith, 1988a). Also of interest is the Rhéoplast®, known as a reliable commercial tool (Vergnes & Villemaire, 1987; Vergnes, Villemaire, Colonna, & Tayeb, 1987), to perform capillary viscometry measurements or to simulate extrusion of starchy products.

Finally, starch melts are commonly considered to exhibit a viscoelastic behavior. The measurement of elastic component of plasticized starch molten phases, associated with the first normal stress difference (N_1), is not trivial because conventional rheometers do not simulate the starch melt created in the extruder. In a recent study using plane-plate geometry, glycerol plasticized starch was shown to behave mainly as a solid-like material, because it was subjected to insufficient mechanical treatment (Della Valle, Buléon, Carreau, Lavoie, & Vergnes, 1998). As an alternative, Senouci and Smith (1988b) related the entrance and exit pressure losses in a slit viscometer die to the elastic properties of potato starch. But, the validity of the exit pressure method have been questioned because flow disturbances, velocity rearrangements or extrudate expansion may affect the stress near the die exit, thus invalidating the fully

Table 2
Rheometrical systems used and shear-rate range covered

Rheometer	Designation	Dimensions	Shear-rate range
Cylindrical die viscometer	CDV	$L/D = 10; 20; 30$, $D = 2$ mm	$10^2 < \dot{\gamma} < 10^4$ s^{-1}
Slit die viscometer	SDV	$L \times W = 210 \times 25$ mm^2, $1 < h < 3$ mm	$1 < \dot{\gamma} < 10^3$ s^{-1}
Pre-shearing rheometer	Rhéoplast®	$L/D = 16; 8; 4; 0.05$, $D = 2$ mm	$10^{-1} < \dot{\gamma} < 10^3$ s^{-1}
Capillary rheometer	Rosand®	$L/D = 16$ and 0.05, $D = 1$ mm	$10^1 < \dot{\gamma} < 5 \times 10^4$ s^{-1}

developed flow assumption, as stated by Ofoli and Steffe (1993) and Padmanabhan and Bhattacharya (1991).

The aim of this work was to determine the viscous behavior of PWS in relation with its transformation, assessed by intrinsic viscosity and thermal analysis. In that purpose, an extruder-fed rheometer was designed and validated with a conventional polymer (LDPE). The viscosity of plasticized molten wheat starch was measured under conditions reflecting the real processing conditions in terms of shear rates, temperature, composition and structural state of the material. The influence of processing conditions on the degradation of starch was evaluated by comparing in-line viscometry measurements with those of the pre-shearing rheometer Rhéoplast. The elastic properties of starch melts were also estimated based on the end pressure effects. This contribution may be useful in predicting the properties of extruded products and determining the processing conditions to reach desired materials specifications.

2. Materials and methods

2.1. Principles and design of the slit and cylindrical die viscometers

A cylindrical die viscometer (CDV) and slit die viscometer (SDV) were designed to be installed at the head of the extruder. As shown in Table 2, a large range of shear rates may be covered, thanks to different die geometries. Fig. 1 presents the schematic of the slit die (SDV). Heating is performed by six 600 W cartridge heaters (3 for each half of die), and temperature control is ensured by thermocouples and closed-loop Eurotherm controllers. The slit die starts with a conical inlet, followed by a rectangular flow channel (slit geometry) with a length (L) of 210 mm, width (W) of 25 mm, and an adjustable height (h) between 1 and 3 mm. The dimensions were chosen so that entrance and edge effects can be neglected (Laun, 1983). The slit die is instrumented with pressure transducers (Dynisco PT462) mounted flush into the fully developed flow zone of the channel, with a decreasing pressure range of 0–607, 0–345 and 0–207 bar, respectively. The temperature probes, mounted on the other half of die, are insulated from the die with a teflon ring. According to Han (1976), the wall shear stress in the SDV is determined by the pressure gradient:

$$\tau_w = \frac{h}{2} \frac{1}{1 + \frac{h}{W}} \frac{dP}{dL} \quad (1)$$

and the apparent wall shear rate is given by:

$$\dot{\gamma}_a = \frac{6Q}{Wh^2} \quad (2)$$

where ΔP is the pressure drop and ΔL the distance between pressure sensors; W, h and L the dimensions of the slit die defined in Fig. 1; and Q the volumetric flow rate (ratio of mass flow-rate and density).

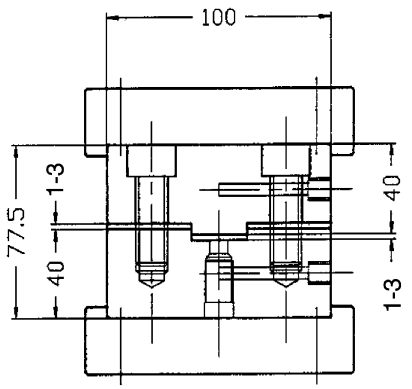

(a)

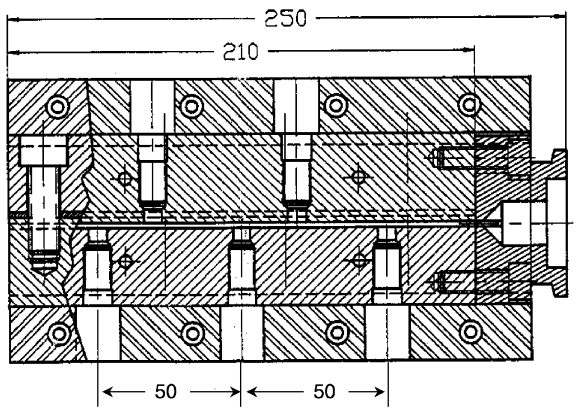

(b)

Fig. 1. Front view (a) and transverse cross-section (b) of the SDV. Dimensions are in mm.

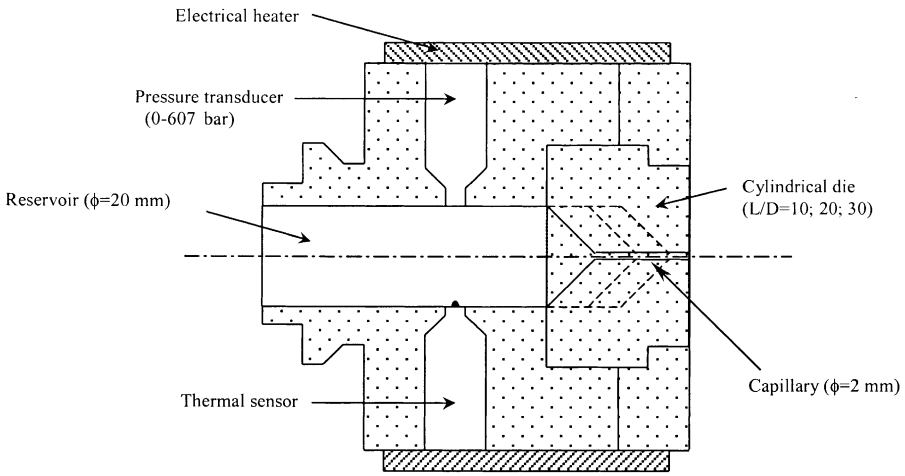

Fig. 2. Cross-section of the CDV. The dashed lines represent the different *L/D* dies.

The Rabinowitch correction is then performed to calculate the real shear rate:

$$\dot{\gamma}_r = \frac{2m+1}{3m}\dot{\gamma}_a \tag{3}$$

with $m = \mathrm{d}(\log \tau_w)/\mathrm{d}(\log \dot{\gamma}_a)$.

Finally, the shear viscosity is given by:

$$\eta(\dot{\gamma}) = \frac{\tau_w}{\dot{\gamma}_r} \tag{4}$$

The CDV consists of a cylindrical reservoir with a diameter of 20 mm (same as the diameter of extruder barrel at the exit) instrumented with a pressure transducer (Dynisco PT462, 0–607 bar) and teflon insulated thermal sensor. The melt stream can then flow through a cylindrical die with a diameter of 2 mm (entry angle of 90°). Various die lengths ($L/D = 10$, 20 and 30) were chosen to determine entrance pressure drops and perform Bagley corrections (Fig. 2). Data treatment is similar to that of capillary rheometry.

2.2. Experimental procedure

The slit die and CDVs were attached to the head of a single-screw extruder. The extruder design was detailed on a previous paper (Martin & Averous, 2001). The extruder and in-line viscometer dies were set in order to reach the desired product temperature. The melt temperature was measured in the flow channel by the teflon-insulated thermal sensor, and also by a portable probe at the exit of die. The temperature of the melt could be maintained to within ±4 °C of the desired product temperature. The shear rate in the instrumented dies was varied either by changing the starch feed-rate, thanks to a K-Tron side feeder, or by increasing the rotation speed of screw (N). The SME delivered to the product was calculated from the hydraulic pressure of the extruder motor drive, given by:

$$\mathrm{SME} = \frac{W - W_0}{Q} = \frac{56N(P_e - P_r) - 2.03N^{2.1785}}{Q} \tag{5}$$

where N is the rotation speed, Q the mass flow rate, and $(P_e - P_r)$ the hydraulic pressure drop in the extruder motor drive. This equation was determined based on the hydraulic motor supplier specifications, and gives an estimation of the SME applied to the product. The term W_0 was determined experimentally, and represents the extruder motor ticking-over energy, described by a power-law function on N.

The mass flow rate was measured by weighing the product at the die exit, at given time intervals. The screw rotation speed and feed-rate were varied together, in the case of starve-fed extrusion, so that the product received similar mechanical treatment at each different flow condition. Measurements of pressure drops and temperatures were made when steady state operation was reached. A graphic recorder was used to measure the pressure change continuously. For each extrusion condition, i.e. with a given melt temperature, plasticizer content and SME level, a dozen values of shear rates in the range (10^1–10^4 s^{-1}) were

Table 3
Compositions of powdery PWS dry-blends and extruded PWS pellets. Each formulation was extruded at 105 °C, at a constant SME level of 400 kWh/t

PWS type	Starch content[a]	Glycerol content[a], GC	Glycerol/starch ratio[a], G/S	Moisture content[a], MC	Density
PWS1	74 (80)	10 (11)	0.14 (0.14)	16 (8.5)	1.39
PWS2	70 (73)	18 (18)	0.26 (0.25)	12 (8.7)	1.37
PWS3	65 (57)	35 (30)	0.54 (0.52)	0 (12.6)	1.34

[a] Compositions of the powdery PWS dry-blends (Pw-PWS) are given in wt% of total wet basis, and values between brackets were determined on extruded PWS pellets (Pe-PWS) after equilibration at 23 °C, 50% RH.

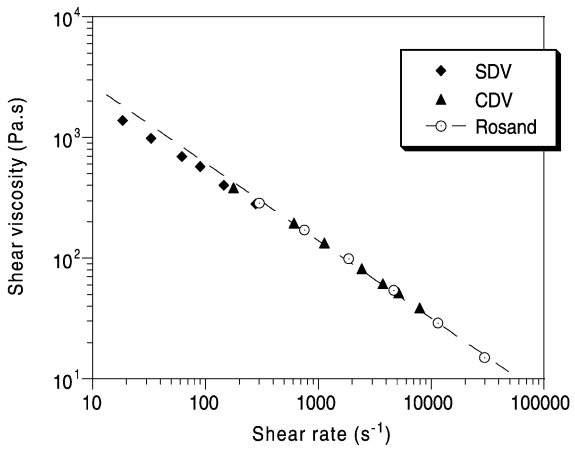

Fig. 3. Overlap of LDPE flow curves at 170 °C obtained from a Rosand® capillary rheometer and from the SDV and CDV extruder-fed rheometers.

obtained. The measurements made with the CDV were repeated for each *L/D* ratio (*L/D* = 10; 20 and 30). Data were recorded and treated according to the procedures mentioned above.

Some experiments were also performed with the pre-shearing rheometer Rhéoplast®, thoroughly described by Vergnes and Villemaire (1987), under the following pre-shearing conditions: $N = 200$ rpm, barrel temperature = 110–150 °C. A conical pre-shearing rheometry was used with a gap of 2.5 mm between the wall and rotating piston. The SME was determined by the torque measurement of rotating piston. Two *L/D* ratios (0.05 and 16) were used and data treatment is performed according to the same principles as capillary viscometry.

2.3. Elastic properties

The entrance and exit flow data can be used to characterize the normal stress difference (N_1). Some authors (Ofoli & Steffe, 1993; Padmanabhan & Bhattacharya, 1991) have used the exit pressure to calculate the first normal stress difference N_1. If the flow in the slit die is assumed to be fully developed, it can be shown that the wall pressure at the exit is related to N_1 by the equation (Han, 1974):

$$N_1 = P_{ex} + \tau_w \left(\frac{\partial P_{ex}}{\partial \tau_w} \right) \quad (6)$$

where P_{ex} is the exit pressure, obtained by extrapolating the pressure measurements along the die to the exit, and τ_w is the shear stress at the die wall.

Another method to evaluate the elastic properties of polymer melts was proposed by Cogswell (1981). Using entrance pressure drop data in a capillary and the flow characteristics, the expression of the elongational viscosity could be derived:

$$\eta_e = \frac{9(m+1)^2(\Delta P_{ent})^2}{32\eta_a \dot{\gamma}_a^2} \quad (7)$$

where m, η_a and $\dot{\gamma}_a$ are the power-law index, apparent viscosity and shear rate, respectively.

The ΔP_{ent} values can be determined either from Bagley plots when a capillary rheometer is used, or by subtracting the extruder barrel head pressure with the extrapolated pressure at the entrance of the die, when a SDV is used.

2.4. Materials preparation

Native wheat starch was purchased from Chamtor (Pomacle, France). The starch contains 74% amylopectin and 26% amylose. According to the supplier, the residual protein and lipids content were less than 0.2% and 0.7%, respectively. Glycerol from ARD (Pomacle, France) with a density of 1.26 and a 99.5 % purity was used as a plasticizer.

Three types of PWS (PWS1, PWS2 and PWS3) with different glycerol/starch ratios, were prepared, as in previous studies (Martin & Averous, 2001). The properties of PWS depend on the amount of plasticizer used. The necessary amounts of glycerol is slowly added to the native starch powder under high-speed mixing, and then placed on

Table 4
Conditions of PWS viscosity measurements (Pw-PWS3, starve-fed mode, SDV viscometry)

No.	Screw speed N (rpm)	Mass flow-rate Q (kg/h)	Entrance pressure P_o (bar)	Die T° T_{die} (°C)	Product T° T_m (°C)	Specific mechanical energy (SME) (kWh/t)
1	60	0.65	130	130	131	641
2	60	1.10	180	130	131	481
3	60	1.45	200	130	132	420
4	60	1.90	235	130	133	396
5	60	2.42	279	130	134	344
6	60	2.89	320	130	134	319
7	20	0.49	148	130	131	335
8	30	1.01	196	130	132	320
9	45	1.55	228	130	133	339
10	60	2.30	292	130	135	327
11	80	3.53	342	130	139	320
12	100	3.85	362	130	141	336

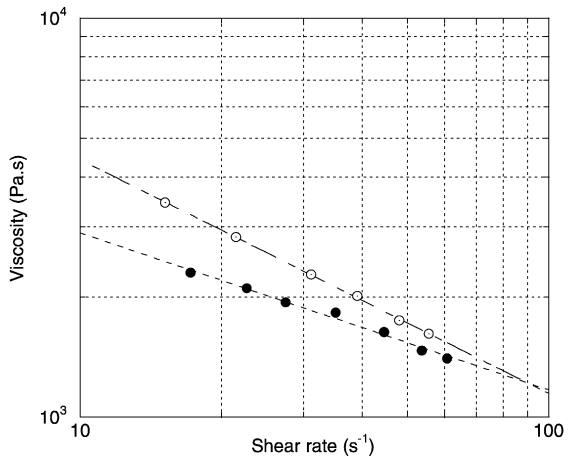

Fig. 4. Influence of the SME on the viscosity values of Pw-PWS3 at 130 °C. Open symbols denote a constant SME treatment (≈325 kWh/t), whereas closed symbols indicate varying SME level (300 < SME < 650 kWh/t).

a vented oven at 170 °C to allow diffusion of glycerol into the starch granule. Then, desired amount of water is added to reach the target composition. The powdery dry-blend prepared can be extruded with a single-screw extruder equipped with a specific high shear and mixing element and extruded in the temperature range of 100–150 °C. The resulting extrudates were pelletized and conditioned at 50% RH and 23 °C, to reach moisture equilibrium. Table 3 shows the different PWS formulations used in the study (starch, water and glycerol contents before and after processing) as well as the SME applied. In the following sections, the Pw-PWS will designate PWS powdery dry-blends, and Pe-PWS will designate the pelletized PWS extrudates.

2.5. Product analysis

The intrinsic viscosity [η] of extruded products was determined at 25 °C in a semi-automatic Schott AVS 400 viscosimeter (solvent flow time, 92 s). A sample of 250 mg of product was stirred for 3 days at room temperature in 10 ml of KOH 1N, and then diluted to 50 ml (KOH 0.2N) to prepare the solution of sample. Then, concentrations ranging from 0.5 to 6 mg/ml were prepared by dilution. Four concentrations were tested for each test sample. Five runs were carried out for each dilution for accuracy purposes. The densities of respective dilutions were measured separately at 25 °C using an Anton-Parr density-meter (DMA60). The intrinsic viscosity was evaluated by extrapolation for zero concentration of the reduced viscosity of solution versus concentration linear curve.

Differential scanning calorimetry (M-DSC 2920, TA instruments, USA) was used to evaluate the residual crystalline structure of PWS extrudates collected after rheological measurements. Water was added on the products to reach a 30% moisture content, and the moist products were allowed to equilibrate for 72 h. The samples were sealed in hermetic aluminum pans to prevent from water volatilization and heated from 0 to 180 °C, at a rate of 5 °C/min. It was checked that limited water volatilization took place by weighing the test samples before and after heating scans.

3. Results and discussion

3.1. Validation with polyethylene

The reliability of the in-line viscometers was first checked with a conventional thermoplastic polymer, a low-density polyethylene (LDPE, ref. 1070MN24 from Atofina), by comparing the viscosity data obtained with those from a Rosand® capillary rheometer. The in-line viscometry experiments were conducted to obtain a flow curve of LDPE at 170 °C. The extruders with slit or cylindrical dies were set to different temperatures in order to reach the targeted product temperature. The temperature of the melt was 168 ± 2 °C. The measurements of LDPE viscosity were carried out regardless the SME, since it has small influence on polyethylene, as stated by Senouci and Smith (1988a). After data treatment, flow curves from both in-line viscometers were drawn, the SDV providing the low-shear data and the CDV providing high-shear data. Fig. 3 shows the viscosity data obtained with both viscometers, as well as the data from the Rosand capillary rheometer. The overlap shows that a good agreement was obtained. The repetition of in-line viscometry measurements showed that the viscosity data of LDPE were reproducible within 3%. Moreover, these preliminary trials have shown that much attention should be taken to perform measurements at stable pressure values (the mean value of recorded signals), and to remain in the linear response domain of the transducers (within 25–80% of the transducer pressure range). Finally,

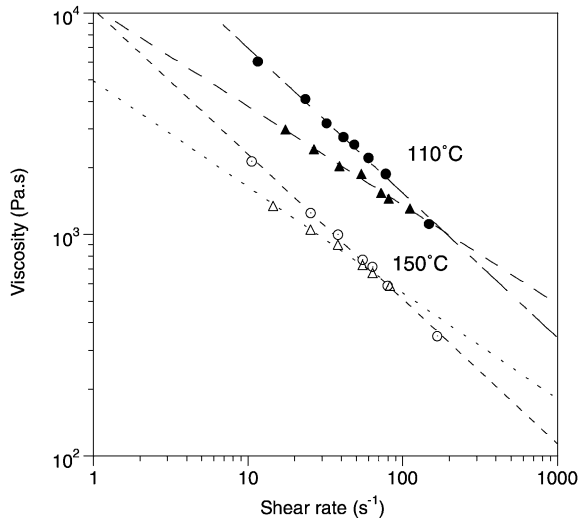

Fig. 5. Viscosity of Pw-PWS3 at 110 and 150 °C for two distinct SME levels (circles represent the standard SME treatment with SME = 300–350 kWh/t, and triangles represent the severe treatment, with SME = 650 kWh/t).

Table 5
Consistency, power-law index and intrinsic viscosity of powdery PWS types obtained under varying processing conditions

No.	Process variables				Parameters		
	Temperature T (°C)	Moisture content MC (w/w)	Glyc. content GC (w/w)	Specific mechanical energy SME (kWh/t)	Consistency K (Pa s)	Power-law index m	Intrinsic viscosity [η] (ml/g)
1	110	12	18	310	54,800	0.35	93
2	110	10	35	355	30,000	0.35	–
3	110	10	35	425	21,700	0.41	–
4	110	10	35	490	16,500	0.43	79
5	110	10	35	540	11,900	0.48	88
6	130	10	10	335	64,200	0.36	100
7	130	12	18	345	32,350	0.39	–
8	130	10	35	350	18,700	0.36	89
9	130	12	18	360	46,200	0.41	100
10	130	20	18	355	19,300	0.44	97
11	150	12	18	325	12,600	0.34	–
12	150	10	35	365	10,350	0.36	81
13	150	10	35	455	3700	0.44	95
14	150	10	35	590	2850	0.54	72
15	150	10	35	650	2500	0.53	76

n.d means the moisture content were not determined.

the temperature regulation of the extruder and dies was always set according to the desired melt temperature of product.

3.2. Experiments with plasticized wheat starch

A first set of experiments was carried out on Pw-PWS3 to select the extrusion conditions for proper viscosity measurements, as reported in Table 4. The criterion for appropriate conditions is a linear pressure profile, stable melt temperature during measurements and constant SME applied to the product. The latter criterion is critical since the SME is known to affect the macromolecular state of starch, and consequently its viscous behavior (Della Valle et al., 1996; Vergnes & Villemaire, 1987). The SME was calculated, at each flow condition, using Eq. (5). The values reported in Table 4 show that, at constant screw speed and increasing feed rate (line 1–6), a large range of SME values may be encountered ($300 < SME < 650$ kWh/t). A fairly constant SME level was obtained (line 7–12, $300 < SME < 350$ kWh/t) by varying the screw speed and feed-rate accordingly, such that the N/Q ratio remains nearly constant during the whole test. In the meantime, the melt temperature raised significantly as the screw speed increased ($\Delta T = 10$ °C). This variation may be attributed to increasing heat dissipation in die, due to higher screw speeds. However, when the rotation speed remains below 60 rpm, the temperature change is limited, and the extrusion conditions thus provide similar thermo-mechanical treatments. Such conditions were fulfilled in further measurement series, because the accuracy of starch viscosity measurements depends directly on the SME and temperature conditions.

PWS follows a typical shear-thinning behavior, and a power law index (m) and consistency (K in Pa s^m) can thus be derived from the experimental data by multiple regression analysis. The flow curves corresponding to experiments of Table 4 are presented in Fig. 4. The K value increased from 7160 to 17,060 Pa s^m and m decreased from 0.60 to 0.41 when the screw speed was varied in order to maintain SME constant. Large values of SME (line 1 and 2), due to lower feed rates at constant screw speed, led to the lower viscosity values. The change in the power law index and consistency clearly indicate the influence of the SME on the starch melt viscosity. Conversely, the higher viscosity values were obtained in the lower SME range, and the viscosity values of both curves were similar at equivalent SME level, i.e. between 320 and 350 kWh/t. These observations support the idea of a larger macromolecular degradation occurring at elevated SME, thus giving rise to lower viscosity values.

From one set of measurements to another, it was possible to change the SME applied to the product by varying the screw filling ratio, i.e. changing the feed-rate in the starve-fed mode. Fig. 5 presents the influence of two different SME treatments on the viscosity of Pw-PWS. Measurements were performed at 110 and 150 °C, for two distinct SME levels, 300–350 kWh/t (standard treatment conditions defined above) and 650 kWh/t (severe treatment). As expected, the consistency of plasticized starch decreased with the intensity of SME, from 31,200 to 10,600 Pa s^m at 110 °C, and from 10,400 to 4900 Pa s^m at 150 °C. From standard to severe treatment, the power law index increased from 0.35 to 0.55 at 110 °C and from 0.35 to 0.52 at 150 °C, respectively. The starch melts became less non-Newtonian as the intensity of treatment increased. The shear history of

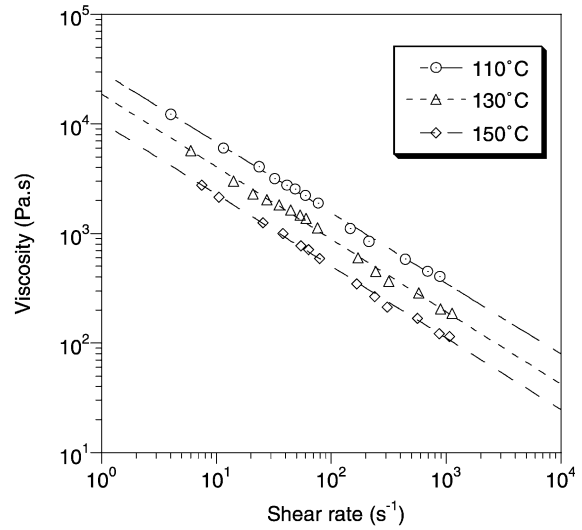

(a)

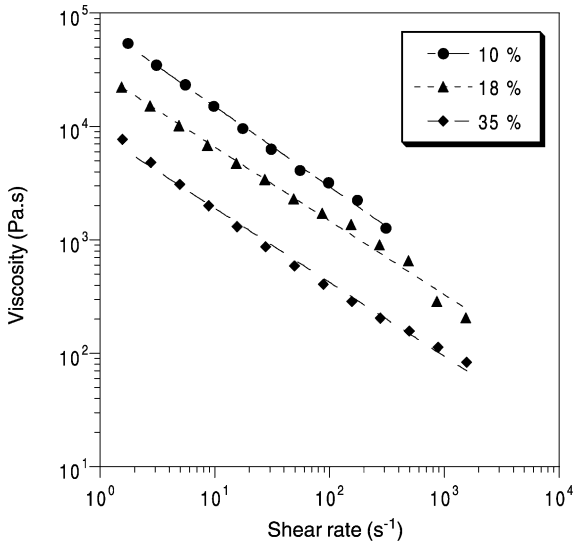

(b)

Fig. 6. Viscosity dependence of PWS on (a) the temperature (variations of Pw-PWS3 are represented at 110, 130 and 150 °C), and (b) the glycerol content (variations of Pe-PWS3 are represented, at 150 °C).

the products is of prime importance since it governs the rheological characteristics. The rheological properties changed during extrusion due to structural modification of starch. However, the shear effects on viscosity appeared more dominant at low temperature. This observation is consistent with the work of Lai and Kokini (1990) who differentiated the contributions of shear and thermal energies in the transformation of starchy products.

3.3. Rheological properties of molten PWS

The effect of temperature, moisture and glycerol content (MC and GC) as well as SME were studied while keeping the other variables constant, as far as practically possible with the SDV and CDV systems. In all cases, the melt viscosity of starch exhibited a pseudoplastic behavior, described by the equation:

$$\eta = K|\dot{\gamma}|^{m-1} \tag{8}$$

Satisfactory continuity in the CDV and SDV viscosity data points was found in the range of shear rates, which is a clear indication that similar thermomechanical treatment was provided in both cases, and that there were no wall slip effect. The consistency and power law index derived from the different conditions tested are compiled in Table 5. The effect of temperature, 110, 130 and 150 °C, on the starch viscosity is presented in Fig. 6a. A small increase in temperature was observed in each set of measurements (about 4–6 °C, from low-shear to high-shear) due to viscous dissipation. The melt viscosity clearly decreased with temperature, and the consistency K gradually decreased

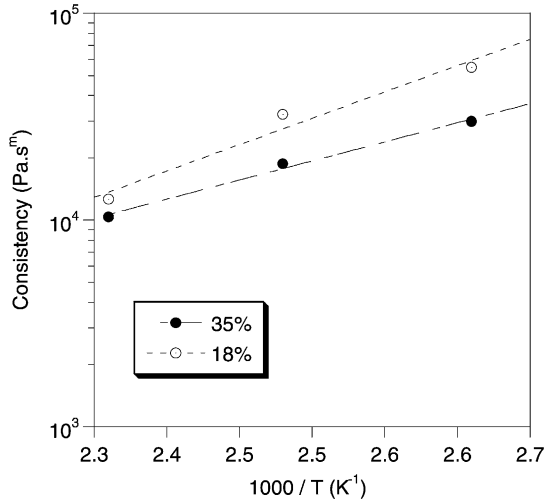

(a)

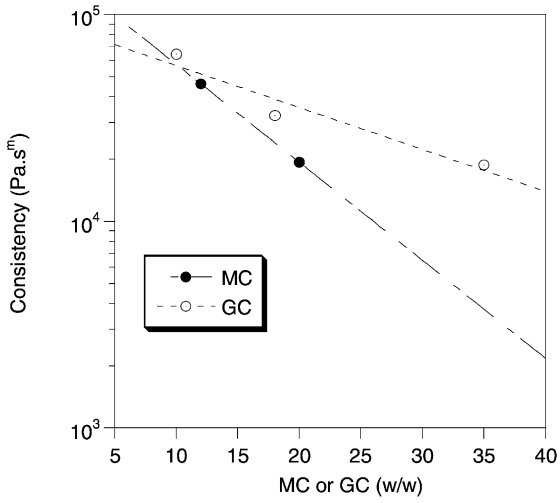

(b)

Fig. 7. Consistency plots of powdery PWS (data from Table 5) versus (a) the reduced temperature, at 18 and 35% glycerol content, and (b) moisture or glycerol contents, at 130 °C.

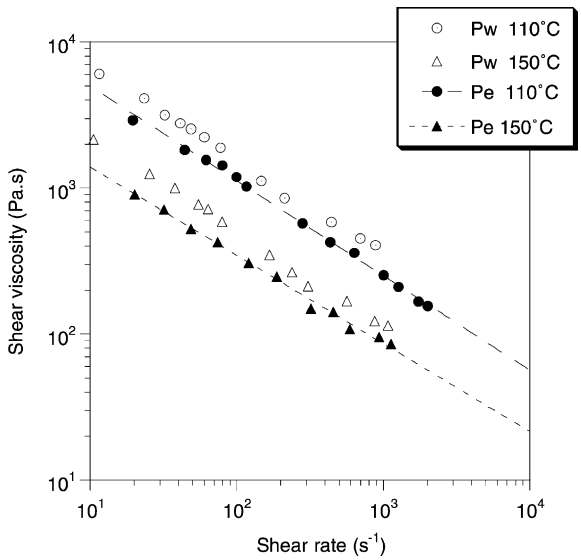

Fig. 8. Comparison between the viscosity curves of Pw-PWS3 (open symbols) and Pe-PWS3 (filled symbols), at 110 and 150 °C.

from 30,000 to 18,700 and 10,350 Pa s^m, for temperatures of 110, 130 and 150 °C, respectively, whereas the change in m (from 0.34 to 0.36) was negligible, within the order of regression analysis error.

Moisture and glycerol contents also have a strong influence on the rheology of starch. As expected, for similar SME conditions (300–350 kWh/t) and moderate temperature rise within set of measures, an increase in moisture and glycerol contents led to a decrease of the consistency K from 46,200 to 19,300 Pa s^m between 12 and 20% MC (lines 9 and 10, Table 5), and from 64,000 to 18,700 Pa s^m between 10 and 35% GC (lines 6–8). The power law index slightly increased with the moisture and glycerol contents, from 0.35 to 0.44. These results are in general agreement with previously published results (Vergnes, Della Valle, & Tayeb, 1993; Vergnes et al., 1987), although Willett, Jasberg, and Swanson (1995) found the power law index decreased, at constant temperature, with increasing moisture contents. In a similar way, the data obtained from the Rhéoplast on Pe-PWS at 150 °C, with pellets moisture content around 10%, show the viscosity decrease with increasing glycerol content (Fig. 6b).

The dependence on moisture and glycerol contents is illustrated by the semi-logarithmic plots of the consistency K versus the temperature or moisture and glycerol (Fig. 7a and b). The consistency K can be expressed as:

$$K = K_0' \exp\left[\frac{E}{R}\left(\frac{1}{T}\right) - \alpha \mathrm{MC} - \alpha' \mathrm{GC}\right] \quad (9)$$

where T is the temperature (in Kelvin), E/R the reduced flow activation energy (K), MC the moisture content and GC the glycerol content (w/w) and K_0 the consistency (Pa s^m).

This equation is similar to those found in literature (Table 1). Linear regression on the consistency plots yielded coefficients of 10.9 for α and 4.7 for α', which confirm the plasticizing effects of moisture and glycerol on starch. The reduced activation energy (E/R) from Fig. 7a are 5860 and 4250 K, for GCs of 18 and 35%.

3.4. Influence of the thermomechanical treatment on starch degradation

The flow curves obtained for powdery and pelletized PWS forms at 110 and 150 °C show significant difference (Fig. 8). This difference may be explained by variations in the total amount of thermomechanical energy delivered, because the Pe-PWS underwent two consecutive extrusion treatments (two passes), versus one single for Pw-PWS. The possible difference in moisture content between the powdery and pelletized PWS may be discarded because PWS pellets were not allowed to equilibrate prior viscometry experiments, so that water uptake was limited. The consistency decreased from 30,000 to 22,200 Pa s^m between Pw-PWS and Pe-PWS at 110 °C, and from 10,350 to 5500 Pa s^m at 150 °C. Again, the increase in temperature changed only the consistency K, values of m (0.35 for all curves) remained within the error margin.

As indicated previously, the thermomechanical treatment applied to plasticized starch affects its viscosity. For instance, in Figs. 4 and 5, increasing SME clearly resulted in a decrease of the PWS viscosity, whatever the PWS type. Thus, the consistency K_0' of Eq. (9) can be expressed with an exponential dependence on the SME, as follows:

$$K_0' = K_0 \exp[-\beta \times \mathrm{SME}] \quad (10)$$

Fig. 9 shows a linear regression on the experimental consistency K values obtained under the different SME conditions reported in Table 5. The scattered points (filled circles) correspond to the plot of K_0' values, whatever the test conditions, whereas the other data points (open circles)

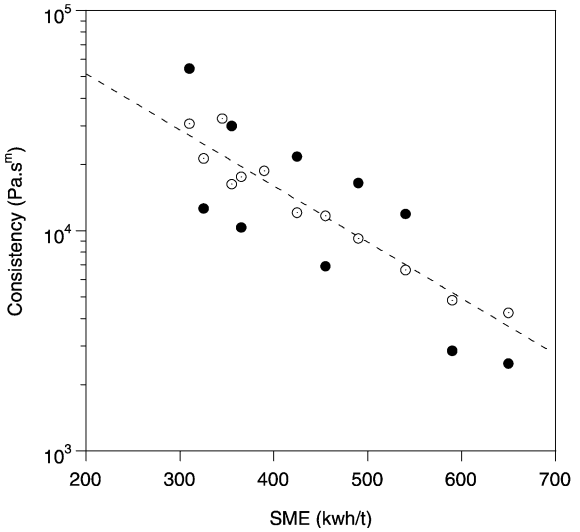

Fig. 9. Consistency values of Pw-PWS versus the SME. The filled circles represent the data obtained under different test conditions (data from Table 5), whereas the open circles were obtained after a temperature correction.

Table 6
Constants from different rheological models of molten starch

Model used	Product	Temperature (°C)	MCs (% w.b.)	K_0 (Pa s^m)	E/R (K)	α	α'	β (kWh/t)$^{-1}$
Vergnes and Villemaire (1987)	Maize	110–170	21–33	7.36	4250	10.6	–	3.1×10^{-3}
Parker et al. (1990)	Corn	100–180	15–32	80.20	4820	26.8	–	3.4×10^{-3}
Willett et al. (1995)	Corn	110–160	15–30	–	8500	12.6	–	–
Della Valle et al. (1995)	Potato	120–180	22–32	0.34	5710	9.45	–	5.4×10^{-3}
Aichholzer and Fritz (1998)*	Corn	130–170	12.5	–	5800	–	6.9	–
Present work	Wheat	100–150	12–20	3.46	5860	10.9	4.7	5.9×10^{-3}

The coefficients E/R and α' were calculated from the original data of the authors.

were obtained after a temperature correction of the same data (except values of lines 6, 9 and 10), to better identify the effect of SME. The β coefficients obtained from the regression of scattered and corrected data points are 6.94×10^{-3} and 5.88×10^{-3} (kWh/t)$^{-1}$, respectively (R^2 of 0.54 and 0.84). This result confirms the effect of SME on the macromolecular degradation of PWS. The accuracy in the determination of the β coefficient is important since small differences of β may lead to large changes of the consistency values.

Eqs. (9) and (10) illustrate the behavior of molten starch and the impact of processing. The following overall model, close to that proposed by Vergnes and Villemaire (1987), accounts for the effects of shear, temperature, moisture and glycerol content and SME:

$$K = K_0 \exp\left[\frac{E}{R}\frac{1}{T} - \alpha \mathrm{MC} - \alpha' \mathrm{GC} - \beta \times \mathrm{SME}\right] \qquad (11)$$

The coefficient obtained for PWS are compared with results from the literature in Table 6. The coefficients found in this work are in good agreement with the values from others studies. The α' coefficient, representing the dependence on GC, allows to better reflect the viscosity of plasticized starch products. The power law index did not vary enough (0.35–0.53) to study accurately its dependence on temperature, moisture content and SME, although Table 5 shows that the increase of some variable induces changes in m as well.

To ascertain the influence of mechanical energy, the viscous behavior of PWS was also measured with the pre-shearing rheometer Rhéoplast®, which has the capacity to subject the product to a well defined thermomechanical treatment prior viscosity measurement. Fig. 10 shows the viscosity curves of Pw-PWS3 obtained from both in-line viscometry and Rhéoplast. At both temperatures, the in-line viscometry data points are approximately a half-decade lower than the Rhéoplast data points. At 130 °C, the consistency K ranged from 56,000 to 18,700 Pa s^m between Rhéoplast and viscometry, and from 39,300 to 10,350 Pa s^m at 150 °C. The power-law index was similar for all curves ($m = 0.34 \pm 0.01$). The explanation of the difference between results obtained from both methods lies in variations in the total SME applied to the product before viscous determination. Moreover, a temperature correction had to be done on the Rhéoplast consistency values, to compare flow curves at the exact same melt temperature.

As shown in Table 7, the shear energy applied to the PWS product in the Rhéoplast is three times lower than the SME encountered in in-line viscometry experiments. It is likely to be sufficient to melt plasticized starch, but macromolecular degradation is certainly less important. By performing corrections on Rhéoplast data (line 2 and 5) in order to adjust with the temperature and SME conditions of in-line viscometry experiments (the E/R and β coefficients from Table 6 were used for the correction of data), satisfactory agreement was found. Thus, the differences between the results of both systems may be ascertained in terms of the modification of starch structure. Moreover, the values of intrinsic viscosity ([η]) reported in Tables 5 and 7 show that an increase in the SME led to a decrease of [η], whatever the additives content. In Fig. 11, the variations of [η] for a wide range of SME values encountered in in-line viscometry ($300 < \mathrm{SME} < 650$ kWh/t) and Rhéoplast experiments ($100 < \mathrm{SME} < 250$ kWh/t) show that the intrinsic viscosity gradually decreased with increasing SME, despite the scattering of data (R^2 of 0.78). This result, explained by the starch macromolecular degradation, is rather confirmatory in nature, and indicates that

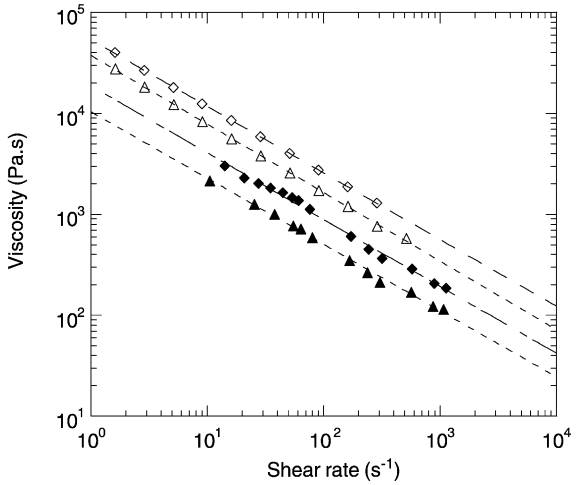

Fig. 10. Comparison between the viscosity curves of Pw-PWS3 at 130 °C (◇ and ◆) and 150 °C (△ and ▲;) obtained with the in-line viscometers and Rhéoplast (open symbols represent Rhéoplast data, and filled symbols represent SDV–CDV data).

Table 7
Comparison of the processing conditions and parameters between viscometry and Rhéoplast

No.	Method	Temperature T (°C)	Specific mechanical energy (SME) (kWh/t)	Consistency K (Pa s^m)	Power-law index m	Intrinsic viscosity [η] (ml/g)
1	Viscometry	130	350	18,700	0.34	89
2	Rhéoplast	130[a]	120	56,000	0.33	118
3	Rhéoplast[b]	130	350	15,000	0.33	–
4	Viscometry	150	365	10,350	0.34	81
5	Rhéoplast	150[a]	120	39,300	0.31	102
6	Rhéoplast[b]	150	365	9200	0.31	–

[a] The temperature indicated is that of barrel section before the die (the real temperature of melt was 10 °C lower).
[b] The Rhéoplast data were corrected to adjust with the temperature and SME of corresponding viscometry data.

the presence of glycerol did not prevent the degradation of starch.

The impact of the applied mechanical treatment on the subsequent structure of PWS was also studied through differential scanning calorimetry (DSC). DSC was performed on samples collected from the Rhéoplast (low SME) and the extruder (high SME range), at a moisture content of 30%. The percentage of added water was chosen to be consistent with previous lab determinations on starch substrates. The thermograms obtained from various PWS3 samples are shown in Fig. 12. The thermogram of native wheat starch (A) exhibits an endotherm at 60 °C corresponding to gelatinization, and a large endotherm around 150 °C, assigned to the melting of the amylopectin, as described by Shogren (1992). The PWS extrudates collected from the Rhéoplast (B and C) were processed at 120 kWh/t, and show endotherms at 60 °C, and small peaks comprised between 120 and 150 °C. Higher temperature endotherms may reflect the melting of residual crystalline native starch structures, or that of crystalline amylose–lipid complexes created during processing in presence of glycerol, as observed by Shogren (1992) and Hulleman, Janssen, and Feil (1998). Similar trend was observed in the case of the extruded samples (D and E), except that the gelatinization endothermic peak became less pronounced as the SME increased, and no other endothermal event was detected at the higher SME level (650 kWh/t). That observation gives the evidence that the crystalline structure of starch gradually disappears as the SME level increases. Thus, at low SME, the starch may not be entirely destructurized, and some native starch granules still remain in the molten mass. At higher SME, an homogeneous starch molten phase may be obtained. Whatever the origin of the PWS structure, i.e. residual crystallites or amylose–lipid complexes, its presence increases the viscosity of PWS, as shown previously. It can be concluded that the intensity of treatment dictates the structural and rheological characteristics of molten starch. However, the depolymerization of PWS mainly due to shear effects and observed through intrinsic viscosity measurements is believed to have a stronger effect than residual crystallinity on the rheology of molten plasticized starch.

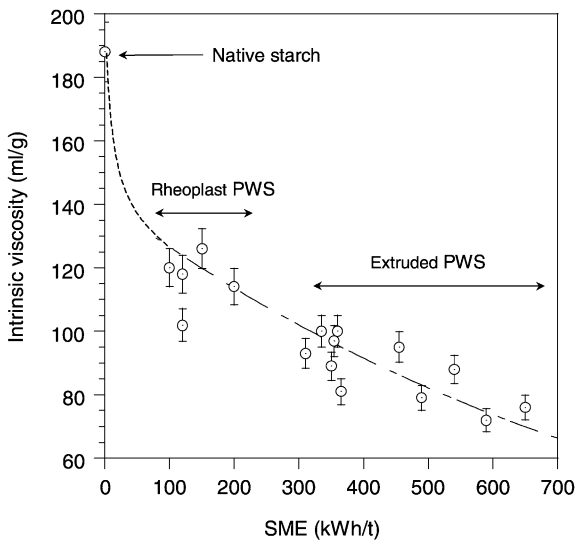

Fig. 11. Intrinsic viscosity [η] as a function of the SME. The data points correspond to products tested through in-line viscometers under various processing conditions (Table 5), and to product tested with the Rhéoplast (Table 7).

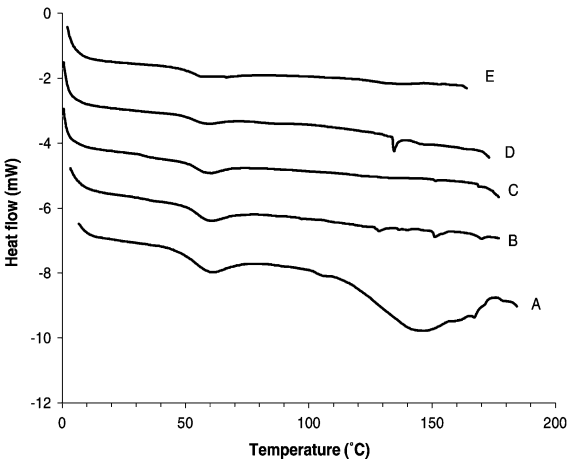

Fig. 12. DSC traces of hydrated PWS3 samples processed in Rhéoplast and in-line viscometers. (A): native wheat starch. (B) and (C): Rhéoplast samples (SME = 120 kWh/t) at 130 and 150 °C. (D) and (E): extruded samples at 350 and 650 kWh/t at 130 °C.

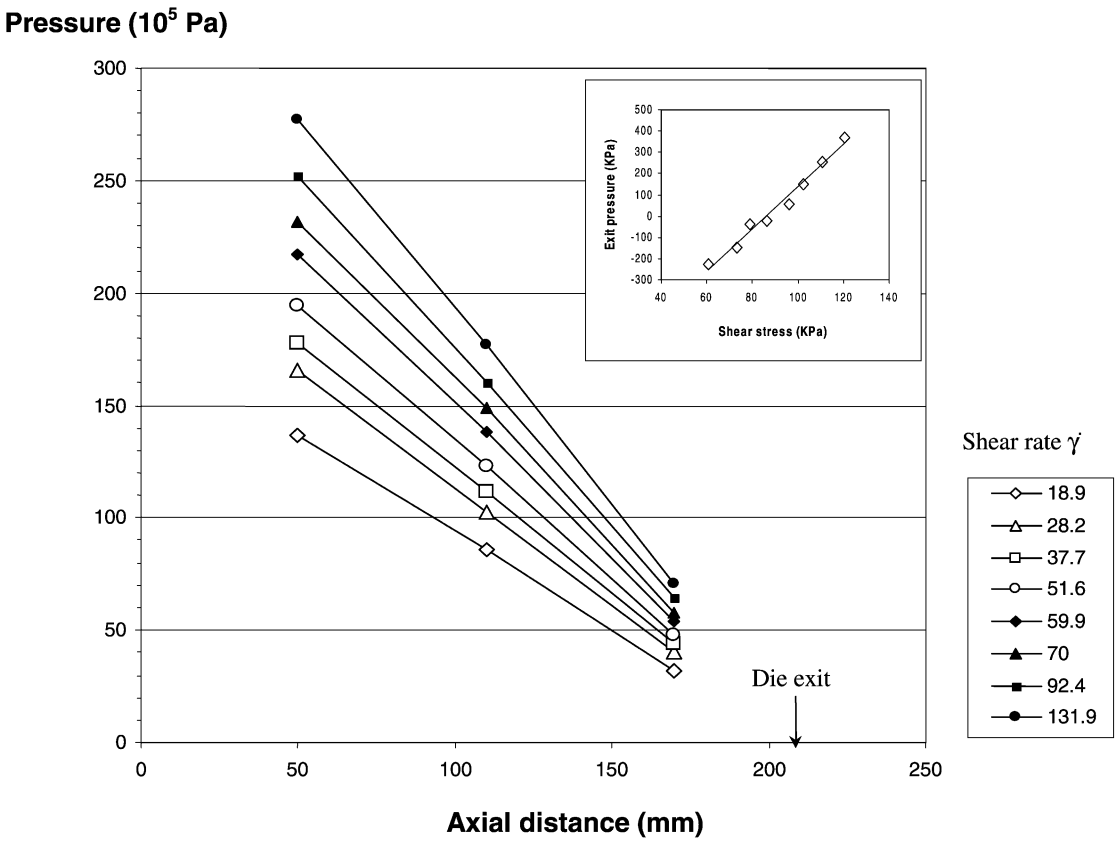

Fig. 13. Pressure profile of Pw-PWS3 at 130 °C under various shear rates. The corresponding exit pressures P_{ex} plot versus shear stress τ_w at 130 °C is shown in the upper right corner.

3.5. Elastic behavior of wheat starch

Instrumented slit and capillary dies attached to the exit of extruders offer the possibility to characterize the elasticity of starchy products. Typical pressure profile obtained with PWS using SDV is presented in Fig. 13, and show that the exit pressures increased with increasing shear stress. The exit pressure values were calculated from linear extrapolations of the pressure values measured in the fully developed flow section of the die, and positive and negative values of P_{ex} were obtained. These values are in agreement with the data reported in the literature. Although the negative exit pressures are physically meaningless, they have been used by some authors (Ofoli & Steffe, 1993; Padmanabhan & Bhattacharya, 1991) to evaluate the elastic properties of starchy products. The exit pressures and N_1 values are presented in Table 8. Contrary to PWS, the P_{ex} values obtained from the linear extrapolation of LDPE pressure profile at 130 °C (data not presented here) decreased with increasing shear rate and shear stress, from

Table 8
Evaluation of the elasticity of Pw-PWS3 at 130 °C using a slit rheometer (SDV) and the Rhéoplast

Exit pressure method (SDV)				Entrance pressure drop (Rhéoplast®)				
Shear rate $\dot{\gamma}$ (s^{-1})	Stress τ_w (kPa)	Exit pressure P_{ex} (kPa)	Elasticity N_1 ($\times 10^5$ Pa)	Shear rate $\dot{\gamma}$ (s^{-1})	Viscosity η_a (kPa s)	Strain rate $\dot{\varepsilon}_A$ (s^{-1})	Elongational viscosity η_e (kPa s)	η/η_e Ratio
18.9	61	−225	3.8	1.9	40.52	0.1	3773	93
28.2	73	−148	5.8	6.0	18.80	0.5	1473	78
37.7	79	−39	7.5	10.6	12.94	0.9	957	74
516	86	−29	8.4	18.8	8.92	1.6	646	72
59.9	96	57	10.2	33.6	6.12	2.8	454	74
70.0	102	149	11.7	59.7	4.17	4.6	344	82
92.4	111	256	13.6	106.2	2.85	8.1	245	85
131.9	120	372	15.7	188.8	1.95	13.5	189	97

200 to − 300 kPa. The exit pressures presented for PWS are similar to those of LDPE. Therefore, the magnitude of PWS exit pressures, related to N_1, indicate that plasticized starch exhibit a non-negligible elastic behavior. Senouci and Smith (1988b) found that potato powder exhibited a high elastic behavior compared to LDPE.

The calculation of elongational viscosity may also be used to evaluate the elastic properties of starch melts. In this work, the ΔP_{ent} values used to calculate η_e were obtained from the Rhéoplast on powdery Pw-PWS3 at 130 °C. The values of apparent elongational and shear viscosity are presented in Table 8. These ratios are in the same range than the values of 60–85 reported by Senouci and Smith (1988b) for maize grits at 120 °C, which may confirm the significant elastic behavior of starch melts. It may be physically meaningful to estimate these ratio at similar rate of deformation, i.e. uniaxial strain rate and shear rate, leading to the ratio $\eta_e(\dot{\varepsilon}_A)/\eta(\dot{\gamma})$. In that case, values of 20 are found. Whatever the method, these results seem to indicate that elongational flow is to be accounted for in extruder die.

4. Conclusion

The viscoelastic properties of PWS were studied using instrumented slit and cylindrical viscometer dies attached to the end of a single-screw extruder, under various extrusion conditions. A large shear rate range ($1-1000\ s^{-1}$) was covered. Experiments with LDPE permitted to validate our in-line viscometry system. The effects of temperature and moisture content on the viscosity of starch were found on the same range as in literature. The plasticizing role of glycerol was also confirmed in a similar manner. The important effect of the thermomechanical treatment (quantified by the SME) was taken into account, and confirmed by the use of a pre-shearing rheometer. In the range of treatments ($200 < SME < 600$ kWh/t), a threefold reduction in viscosity was found, thus indicating the importance of processing. A general rheological model, similar to that reported by other authors, was used to integrate the effects of temperature, plasticizer content (MC and GC) and thermomechanical treatment (SME). The coefficients found are in good agreement with those of literature. The influence of SME on the degradation of starch products, collected after SDV and Rhéoplast experiments, has been evaluated by intrinsic viscosity measurements and thermal analysis. The gradual decrease of [η] with increasing SME confirmed that macromolecular degradation had occurred, whatever the PWS composition, and DSC thermograms gave some evidence of crystalline organization remaining in processed PWS. Finally, the entrance and exit pressure effects were used to evaluate the elasticity of the melt. These data lead to the conclusion that significant elastic properties may be expected from PWS.

More work, however, may be necessary to understand the relationship between the molecular structure of extruded starch products and their functional properties. Furthermore, the elastic behavior of thermoplastic starches need to be more completely addressed for processing applications.

Acknowledgements

This work was funded by Europol'Agro through a research program devoted to the development of packaging materials based on agricultural resources. The authors wish to thank Bruno Liesch and Pascal Vasseur (University of Reims) for useful technical assistance.

References

Aichholzer, W., & Fritz, H. S. (1998). Rheological characterization of thermoplastic starch materials. *Starch/Stärke*, *2–3*, 77–83.

Barrès, C., Vergnes, B., Tayeb, J., & Della Valle, G. (1990). Transformation of wheat flour by extrusion cooking: Influence of screw configuration and operating conditions. *Cereal Chemistry*, *67*, 427–433.

Bastioli, C., Bellotti, V., & Rallis, A. (1994). Microstructure and melt flow behavior of a starch-based polymer. *Rheologica Acta*, *33*, 307–316.

Cervone, N. W., & Harper, J. M. (1978). Viscosity of an intermediate moisture dough. *Journal of Food Processing Engineering*, *2*, 83-95.

Cogswell, F. N. (1981). *Polymer melt rheology*. London: George Godwin.

Colonna, P., Tayeb, J., & Mercier, C. (1989). Extrusion-cooking of starch and starchy products. In C. Mercier, P. Linko, & J. M. Harper (Eds.), *Extrusion-cooking* (pp. 247–320). St Paul: AACC.

Davidson, V. J., Paton, D., Diosady, L. L., & Larocque, G. J. (1984a). Degradation of wheat starch in a single-screw extruder: Characteristics of extruded starch polymers. *Journal of Food Science*, *49*, 453–458.

Davidson, V. J., Paton, D., Diosady, L. L., & Rubin, L. T. (1984b). A model for mechanical degradation of wheat starch in a single-screw extruder. *Journal of Food Science*, *49*, 1154–1169.

Della Valle, G., Boché, Y., Colonna, P., & Vergnes, B. (1995). The extrusion behaviour of potato starch. *Carbohydrate Polymers*, *28*, 255–264.

Della Valle, G., Buléon, A., Carreau, P. J., Lavoie, P.-A., & Vergnes, B. (1998). Relationship between structure and viscoelastic behavior of plasticized starch. *Journal of Rheology*, *42*, 507–525.

Della Valle, G., Colonna, P., Patria, A., & Vergnes, B. (1996). Influence of amylose content on the viscous behavior of low hydrated molten starches. *Journal of Rheology*, *40*, 347–362.

Doane, W. M. (1992). USDA research on starch-based biodegradable plastics. *Starch/Stärke*, *44*, 293–295.

Fletcher, S. I., Mc Master, T. J., Richmond, P., & Smith, A. C. (1985). Rheology and extrusion of maize grits. *Chemical Engineering Communications*, *32*, 239–261.

Han, C. D. (1974). On slit- and capillary-die rheometry. *Journal of Rheology*, *18*, 163–190.

Han, C. D. (1976). *Rheology in polymer processing*. New York: Academic Press.

Harper, J. M., Rhodes, T. P., & Wanninger, L. A. (1971). Viscosity model for cooked cereal doughs. AIChE symposium. *67*, 40–43.

Hulleman, S. H. D., Janssen, F. H. P., & Feil, H. (1998). The role of water during plasticization of native starches. *Polymer*, *39*, 2043–2048.

Lai, L. S., & Kokini, J. L. (1990). The effect of extrusion operating conditions on the on-line apparent viscosity of 98% amylopectin (Amioca) and 70% amylose (Hylon) corn starches during extrusion. *Journal of Rheology*, *34*, 1245–1266.

Laun, H. M. (1983). Polymer rheology with a slit die. *Rheologica Acta*, *22*, 171–185.

Martin, O., & Averous, L. (2001). Poly(lactic acid): Plasticization and properties of biodegradable multiphase systems. *Polymer*, *42*, 6209–6219.

McMaster, T. J., Senouci, A., & Smith, A. C. (1987). Measurement of rheological and ultrasonic properties of food and synthetic polymer melts. *Rheologica Acta*, *26*, 308–315.

Ofoli, R. Y., & Steffe, J. F. (1993). Some observations on the use of slit rheometry for characterizing the primary normal stress difference of extrudates. *Journal of Food Engineering*, *18*, 145–157.

Padmanabhan, M., & Bhattacharya, M. (1991). Flow behavior and exit pressures of corn meal under high-shear-high-temperature extrusion conditions using a slit die. *Journal of Rheology*, *35*, 315–343.

Parker, R., Ollett, A. L., Lai-Fook, R. A., & Smith, A. C. (1990a). *The rheology of food 'melts' and its application to extrusion processing*. *Rheology of food, pharmaceutical and biological materials*, London: R.E. Carter, pp. 53–69.

Parker, R., Ollett, A. L., & Smith, A. C. (1990b). *Starch melt rheology: Measurements, modelling and application to extrusion processing*. *Processing and quality of foods*, London: P. Zeuthen, pp. 1290–1295.

Senouci, A., & Smith, A. C. (1988a). An experimental study of food melt rheology. I. Shear viscosity using a slit die and a capillary rheometer. *Rheologica Acta*, *27*, 546–554.

Senouci, A., & Smith, A. C. (1988b). An experimental study of food melt rheology. II. End pressure effects. *Rheologica Acta*, *27*, 649–655.

Shogren, R. L. (1992). Effect of moisture content on the melting and subsequent physical aging of cornstarch. *Carbohydrate Polymers*, *19*, 83–90.

Vergnes, B., Della Valle, G., & Tayeb, J. (1993). A specific slit die rheometer for extruded starchy products. Design, validation and application to maize starch. *Rheologica Acta*, *32*, 465–476.

Vergnes, B., & Villemaire, J. P. (1987). Rheological behaviour of low moisture maize starch. *Rheologica Acta*, *26*, 570–576.

Vergnes, B., Villemaire, J. P., Colonna, P., & Tayeb, J. (1987). Interrelationships between thermomechanical treatment and macromolecular degradation of maize starch in a novel rheometer with preshearing. *Journal of Cereal Science*, *5*, 189–207.

Willett, J. L., Jasberg, B. K., & Swanson, C. L. (1995). Rheology of thermoplastic starch: effects of temperature, moisture content, and additives on melt viscosity. *Polymer Engineering and Science*, *35*, 202–210.

Zheng, X. Z., & Wang, S. W. (1994). Shear induced starch conversion during extrusion. *Journal of Food Science*, *59*, 1137–1143.